Development/Plasticity/Repair

Subregional Specification of Embryonic Stem Cell-Derived Ventral Telencephalic Tissues by Timed and Combinatory Treatment with Extrinsic Signals

Teruko Danjo,[1,2] Mototsugu Eiraku,[1] Keiko Muguruma,[1] Kiichi Watanabe,[1] Masako Kawada,[1] Yuchio Yanagawa,[3] John L. R. Rubenstein,[4] and Yoshiki Sasai[1,2]

[1]Organogenesis and Neurogenesis Group, Center for Developmental Biology, RIKEN, Kobe 650-0047, Japan, [2]Department of Medical Embryology, Graduate School of Medicine, Kyoto University, Kyoto 606-8501, Japan, [3]Department of Genetic and Behavioral Neuroscience, Gunma University Graduate School of Medicine, Maebashi 371-8511, Japan, and [4]Center for Neurobiology and Psychiatry, University of California, San Francisco, School of Medicine, San Francisco, California 94158-2324

During early telencephalic development, the major portion of the ventral telencephalic (subpallial) region becomes subdivided into three regions, the lateral (LGE), medial (MGE), and caudal (CGE) ganglionic eminences. In this study, we systematically recapitulated subpallial patterning in mouse embryonic stem cell (ESC) cultures and investigated temporal and combinatory actions of patterning signals. In serum-free floating culture, the dorsal-ventral specification of ESC-derived telencephalic neuroectoderm is dose-dependently directed by Sonic hedgehog (Shh) signaling. Early Shh treatment, even before the expression onset of Foxg1 (also Bf1; earliest marker of the telencephalic lineage), is critical for efficiently generating LGE progenitors, and continuous Shh signaling until day 9 is necessary to commit these cells to the LGE lineage. When induced under these conditions and purified by fluorescence-activated cell sorter, telencephalic cells efficiently differentiated into Nolz1$^+$/Ctip2$^+$ LGE neuronal precursors and subsequently, both in culture and after *in vivo* grafting, into DARPP32$^+$ medium-sized spiny neurons. Purified telencephalic progenitors treated with high doses of the Hedgehog (Hh) agonist SAG (Smoothened agonist) differentiated into MGE- and CGE-like tissues. Interestingly, in addition to strong Hh signaling, the efficient specification of MGE cells requires Fgf8 signaling but is inhibited by treatment with Fgf15/19. In contrast, CGE differentiation is promoted by Fgf15/19 but suppressed by Fgf8, suggesting that specific Fgf signals play different, critical roles in the positional specification of ESC-derived ventral subpallial tissues. We discuss a model of the antagonistic Fgf8 and Fgf15/19 signaling in rostral-caudal subpallial patterning and compare it with the roles of these molecules in cortical patterning.

Introduction

During early mammalian development, the embryonic telencephalon subdivides into the dorsal telencephalon (pallium) and the ventral telencephalon (subpallium). The latter is further specified to form three ganglionic eminences, the septum, and the ventralmost telencephalic stalk regions (e.g., the preoptic and anterior entopeduncular areas) (Marin and Rubenstein, 2002; Flames et al., 2007). The ganglionic eminences consist of the lateral ganglionic eminence (LGE) (rostral-dorsal in the subpallium), the medial ganglionic eminence (MGE) (rostral-ventral), and the caudal ganglionic eminence (CGE) (caudal). The LGE and MGE generate the two large nuclei in the telencephalic basal ganglia, the striatum and the globus pallidus, respectively, which play central roles in motor control and coordination via the extrapyramidal system. In addition to contributing to these subpallial structures, a substantial portion of the MGE and CGE derivatives migrate dorsally and give rise to cortical interneurons (Deacon et al., 1994; Olsson et al., 1995, 1998; Anderson et al., 1997, 2001; Lavdas et al., 1999; Sussel et al., 1999; Wichterle et al., 2001; Nery et al., 2002; Xu et al., 2004; Butt et al., 2005; Wonders and Anderson, 2006; Miyoshi et al., 2007; Flandin et al., 2010).

Previous studies have demonstrated the importance of patterning signaling via Sonic hedgehog (Shh) in subpallial development (Chiang et al., 1996; Shimamura and Rubenstein, 1997; Fuccillo et al., 2004; Xu et al., 2005, 2010). A *Shh*-null mouse forms morphologically defective ganglionic eminences with severely reduced subpallial markers including Nkx2.1 (Ohkubo et al., 2002). A conditional loss of *Shh* from an early stage [approximately embryonic day 8.5 (E8.5)] causes severe defects of all ventral telencephalic tissues (Fuccillo et al., 2004). In contrast, a conditional *Shh* knock-out (around E10–E12) results in only

Received Sept. 30, 2010; revised Nov. 22, 2010; accepted Dec. 1, 2010.

This work was supported by grants-in-aid from the Ministry of Education, Culture, Sports, Science and Technology (Y.S., M.E.), the Kobe Cluster Project (Y.S.) and the Leading Project (Y.S.), the National Center of Neurology and Psychiatry (K.M.), and the Japan Science and Technology Agency (Y.Y.; Core Research for Evolutional Science and Technology). We are grateful to Kazuaki Yoshikawa for the Dlx2 antibody, to Drs. Arturo Alvarez-Buylla, Arnold Kriegstein, Scott Baraban, and Jeremy Reiter for their stimulating discussion and invaluable advice, to Dr. Makoto Nasu for critical reading, and to members of the Sasai Laboratory for discussion and advice.

Correspondence should be addressed to either Dr. Mototsugu Eiraku or Dr. Yoshiki Sasai, Organogenesis and Neurogenesis Group, Center for Developmental Biology, RIKEN, 2-2-3 Minatojima-minamimachi, Chuo, Kobe 650-0047, Japan. E-mail: eiraku@cdb.riken.jp or yoshikisasai@cdb.riken.jp.

DOI:10.1523/JNEUROSCI.5128-10.2011

 0270-6474/11/311919-15$15.00/0

limited defects in ventral telencephalic patterning (Xu et al., 2005). These findings suggest that Shh signaling during early telencephalic development plays a critical role in subpallial development.

In our previous studies, we showed that embryonic stem cells (ESCs) can be steered to differentiate into telencephalic progenitors when cultured as floating aggregates in a growth factor-minimized serum-free medium (serum-free floating culture of embryoid body-like aggregates with quick reaggregation, hereafter SFEBq culture) (Watanabe et al., 2005; Eiraku et al., 2008). They can form laminar structures similar to the marginal zone, the early cortical-plate zone, the basal-progenitor zone, and the ventricular zone (Eiraku et al., 2008). The directed differentiation of ESC-derived neural progenitors into telencephalic neurons has been also reported using other culture systems, including adhesion culture (Gaspard et al., 2008; Li et al., 2009; Ideguchi et al., 2010).

Our previous study demonstrated that treating ESC-derived telencephalic cells with Shh promotes subpallial differentiation at the expense of pallial differentiation (Watanabe et al., 2005). However, the analysis was qualitative and the mode of subpallial commitment, particularly along the time axis, has remained elusive. In this study, we sought to understand the temporal and combinatory regulations by extracellular signals in the region-specific differentiation of ESC-derived subpallial precursors. We first investigated the stage-dependent action of Shh signaling (see Figs. 1–4), and then asked what other factors interact or cooperate with Shh to specify cells to particular subpallial subregions *in vitro* (see Figs. 5, 6).

Materials and Methods

Embryonic stem cell culture. Mouse *Foxg1::venus* ESCs (EB3-derived) were maintained as described previously (Watanabe et al., 2005). For differentiation, G-MEM medium was supplemented with 10% Knock-Out Serum Replacement (KSR) (Invitrogen), 2 mM glutamate, 1 mM pyruvate, 0.1 mM nonessential amino acids, 0.1 mM 2-ME (2-mercaptoethanol), and 200 ng/ml Dkk-1. For SFEBq culture [modified from the study by Eiraku et al. (2008)], ESCs were dissociated to single cells in 0.25% trypsin-EDTA and quickly reaggregated in the differentiation medium (5000 cells/80 μl/well) using 96-well low cell adhesion plates (Lipidure Coat from NOF or PrimeSurface 96U plate from Sumilon). On day 6, cell aggregates were transferred to a 10 cm bacterial-grade dish with N2 medium (DMEM/F12 supplemented with N2). Differentiation day 0 was defined as the day on which ESCs were seeded to differentiate. All recombinant proteins were purchased from R&D Systems. *N*-[2-[[4-(Diethylamino)butyl]amino]-6-(3,5-dimethoxyphenyl)pyrido[2,3-*d*]pyrimidin-7-yl]-*N*′-(1,1-dimethylethyl)urea (PD173074) was purchased from Calbiochem.

For cortical-type differentiation, cyclopamine (BIOMOL; 5 μM) was added on day 8. For LGE-type differentiation, 10 nM Shh was added on day 3, and again on day 6. For MGE-type differentiation, Shh was added at 10 nM on day 3 and at 30 nM on day 6, or Smoothened agonist (SAG) (Alexis Biochemicals) was added at 3 nM on day 3 and at 10 nM on day 6.

Immunohistochemistry. Immunohistochemistry was performed as described previously (Watanabe et al., 2005). Foxg1::venus signals were detected using an anti-green fluorescent protein (GFP) antibody (rabbit, 1:500; MBL; rat, 1:500; Nacalai Tesque; chick, 1:500; Aves Labs). Polyclonal antiserum against mouse Nolz1 was obtained by immunizing guinea pigs with the synthetic peptide KDAKSGPLKLSDIGC and used after protein A purification. Other primary antibodies were against Foxg1 (rabbit; 1:5000) (Watanabe et al., 2005); Gsh2 (guinea pig, 1:500; rabbit, 1:10,000) (Watanabe et al., 2005); Nkx2.1 (rabbit, 1:2000; Biopat; mouse, 1:500; Novocastra); Pax6 (rabbit, 1:500; Covance; mouse, 1:200; Developmental Studies Hybridoma Bank; goat, 1:100; Santa Cruz); Dlx2 (guinea pig, 1:5000; a kind gift from Kazuaki Yoshikawa, Osaka University, Osaka, Japan); GAD67 (mouse, 1:1000; Millipore Bioscience Research Reagents); GAD65/67 (rabbit, 1:50,000; Sigma-Aldrich); Tbr1 (rabbit, 1:1000; Chemicon); Nolz1 (guinea pig; 1:500); Ctip2 (rat, 1:500; Abcam); Foxp1 (rabbit, 1:10,000; Abcam); DARPP32 (rabbit, 1:2000; Santa Cruz; mouse, 1:1000; BD Biosciences Pharmingen); Bassoon (mouse, 1:400; Assay Designs); somatostatin (SOM) (rat, 1:100; Millipore Bioscience Research Reagents); neuropeptide Y (NPY) (rabbit, 1:1000; Immunostar); parvalbumin (PV) (rabbit, 1:5000; Abcam); CoupTFII (mouse, 1:1000; Perseus Proteomics); calbindin (rabbit, 1:500; Millipore Bioscience Research Reagents); CD133 (rat, 1:500; Millipore Bioscience Research Reagents); Ikaros (rabbit, 1:100; Santa Cruz); Ki67 (mouse, 1:200; BD Biosciences Pharmingen); Tuj1 (rabbit, 1:500; Covance); GFAP (rabbit, 1:1000; Millipore Bioscience Research Reagents); Sox1 (rabbit, 1:200; Cell Signaling); phosphohistone H3 (rabbit, 1:200; Millipore); calretinin (CAR) (rabbit, 1:5000; Swant); and GABA (rabbit, 1:5000; Sigma-Aldrich). Images were acquired with a confocal microscope (LSM 710; Zeiss). Quantification was conducted using the vHCS Discovery Toolbox software (Thermo Fisher Scientific). Values shown in graphs represent the mean ± SE. For quantitative analysis, 12–24 aggregates were examined for each experiment, which was repeated at least three times, unless otherwise noted.

Quantitative PCR. Quantitative PCR (qPCR) was performed using the 7500 Fast Real-Time PCR system (Applied Biosciences), and the data were normalized to the glyceraldehyde-3-phosphate dehydrogenase (GAPDH) expression. The primers used for qPCR were as follows: GAPDH, 5′-tgaccacagtccatgccatc and 5′-gacggacacattgggggtag; Lhx6, 5′-ctacttcagccgatttggaacc and 5′-gcaaagcactttctcctcaacg; gli1, 5′-ccaagccaactttatgtcaggg and 5′-agcccgcttctttgttaatttga; fgf8, 5′-gtcctgcctaaagtcacacag and 5′-cttccaaaagtatcggtctccac; fgf15, 5′-ggcaagatatacgggctgat and 5′-tccatttcctccctgaaggt. Values shown in graphs represent the mean ± SE. For quantitative analysis, each experiment was repeated at least three times unless otherwise noted.

Fluorescence-activated cell sorter sorting and reaggregation culture. For fluorescence-activated cell sorter (FACS) analysis, cells were counted with a FACSAria (BD Biosciences), and the data were analyzed with the FACSDiva software (BD Biosciences). *Foxg1::venus* ESC aggregates were dissociated to single cells using the Neural Tissue Dissociation Kit (Sumilon), and filtered through a Cell Strainer (BD Biosciences), and analyzed at 4°C. Sorted cells were collected in ice-cold DMEM/F12/N2/10% FBS and quickly reaggregated in DMEM/F12/N2/2% FBS using 96-well low cell adhesion plates (2×10^4 cells/well). One-half of the medium volume was changed every 3 d after sorting.

Dissociation neuronal culture. For dissociation culture, the sorted Foxg1::venus$^+$ cell aggregates were dissociated using the Neural Tissue Dissociation Kit (Sumilon) on day 13, and plated onto poly-D-lysine-coated dishes at a density of 1×10^5 cells/cm^2 in DMEM/F12/N2/10% FBS. On the next day of plating, the medium was changed to Neuron Culture Medium (Sumilon), which contains rat glial conditioned medium. On day 21, the medium was changed to Neurobasal/B27 supplemented with 20 ng/ml BDNF and 20 ng/ml NT3. Thereafter, one-half of the volume of the medium was changed every 5 d.

Transplantation. To prepare LGE-type Foxg1::venus$^+$ cells for transplantation, SFEBq aggregates were treated with 10 nM Shh from days 3–9, sorted on day 9, and treated with 10 nM Shh after sorting. Similar results were obtained by treating the cells with 6 nM Shh during days 3–9, sorting on day 9, and treating with 30 nM Shh after sorting. Reaggregates of sorted Foxg1::venus$^+$ cells were cultured for 4 additional days, and dispersed with the Neural Tissue Dissociation Kit (Sumilon). Transplantation was performed by anesthetizing day 2 postnatal ICR mice on ice for 3 min, exposing the skull, and injecting the cell suspension ($1–2 \times 10^6$ cells per 3 μl) into the striatum (coordinated 1 mm anterior, 1 mm lateral, and 2.5 mm deep from the bregma) or the cortical plate (2 mm deep). The pups were revived by warming at 36°C and returned to the litter. The animals were cared for in accordance with the Regulations on Animal Experiments of RIKEN. For analysis, host mice were perfused transcardially with 4% paraformaldehyde, and 50 μm-thick brain sections were taken for immunostaining.

Brain slice coculture. Coronal sections (250 μm thick) of the brains excised from E13.5 mice were prepared using vibratome (ZERO 1; DSK). Foxg1::venus$^+$ cell aggregates were cultured under MGE conditions

(treated with 3 nM SAG during days 3–6, with 10 nM SAG during days 6–8, and sorted on day 8). On day 15, Foxg1::venus$^+$ reaggregates were isolated into an appropriate size under a fluorescence dissecting microscope, and the cell masses were inserted into the subventricular zone of the forebrain slices, which were cocultured for 3 d on a Transwell culture insert (Corning) containing slice culture medium (DMEM/F12/N2/10% FBS) under a 40% O_2/5% CO_2 condition.

Results

Selective induction of cortex-, LGE-, and MGE-type differentiation by different levels of Shh signals in SFEBq culture

Both the pallium and subpallium of the developing telencephalon (Fig. 1*A–D*) express the region-specific transcription factor Foxg1 (Fig. 1*A*). The neuroepithelium of the cortex strongly expresses Pax6, whereas that of the subpallium expresses Gsh2 (also called Gsx2) (Stoykova and Gruss, 1994; Hsieh-Li et al., 1995; Toresson et al., 2000; Yun et al., 2001) (higher expression in the LGE than in the MGE). In the subpallium, Nkx2.1 is expressed in the MGE and preoptic area, but not in the LGE or CGE (Fig. 1*B*,*D*) (Shimamura et al., 1995; Sussel et al., 1999). In addition, neurons derived from the pallium or subpallium are distinguished by specific molecular markers. Early-born cortical neurons express Tbr1, whereas Dlx2 is expressed in subpallium-derived neurons (Fig. 1*C*,*D*) (Bulfone et al., 1993, 1995; Porteus et al., 1994; Anderson et al., 1997; Long et al., 2009a,b). The majority of subpallium-derived neurons are GABAergic and express GAD67, in contrast to pallium-derived neurons, which are mostly glutamatergic (Fig. 1*C*,*D*) (Hevner et al., 2001; Gorski et al., 2002; Stühmer et al., 2002).

We first tested whether the dorsal-ventral specification of telencephalic progenitors could be controlled in an SFEBq culture by regulating Shh dosage, and whether SFEBq culture could generate and maintain neuroepithelial structures from ESC-derived subpallial progenitors, as it does in the case of ESC-derived pallial neuroepithelium.

In the absence of exogenous Shh signals, SFEBq-cultured ESC aggregates differentiate preferentially into cortical progenitors (Eiraku et al., 2008). When Shh signaling was blocked by the Hedgehog (Hh) inhibitor cyclopamine from day 8 onward (condition 1) (Fig. 1*E–I*), the majority of ESC-derived Foxg1$^+$ telencephalic cells expressed the cortical markers Pax6 or Tbr1 on day 12, whereas few expressed Gsh2, Nkx2.1, Dlx2, or GAD67. However, a moderate dose of Shh (10 nM) (condition 2) (Fig. 1*J–M*) strongly inhibited differentiation into Pax6$^+$ or Tbr1$^+$ cortical cells, and the ESC-derived Foxg1$^+$ telencephalic cells expressed the subpallial markers Gsh2, Dlx2, or GAD67. Although the MGE marker Nkx2.1 was seen infrequently in cells cultured with a moderate dose of Shh (10 nM), the aggregates treated with a higher concentration (30 nM) contained a substantial number of Nkx2.1$^+$ cells (condition 3) (Fig. 1*N–Q*). The Hedgehog agonist SAG, which induced the Shh target gene *Gli1* at least a few times more potently than recombinant Shh at the same concentrations (supplemental Fig. 1*F*,*G*, available at www.jneurosci.org as supplemental material) (Chen et al., 2002), also efficiently increased Nkx2.1 expression (supplemental Fig. 1*H–N*, available at www.jneurosci.org as supplemental material). The quantitative data for marker expressions, obtained by immunostaining, are shown in Figure 1*R–U*. FACS analysis using ESCs with GFP (venus) knocked-in at the *Foxg1* locus showed that the percentage of Foxg1::venus$^+$ cells was not affected by Shh or cyclopamine treatment (supplemental Fig. 1*A–D*, available at www.jneurosci.org as supplemental material).

As in the case of cortical differentiation (Fig. 1*G*), Shh-treated aggregates formed neural rosettes, indicating that the neuroepithelial structure was maintained at least to some extent in this culture (Fig. 1*L*,*P*,*Q*; supplemental Fig. 1*E*, available at www.jneurosci.org as supplemental material). Within the rosettes, mitotically active Gsh2$^+$ progenitors (also Ki67$^+$) (data not shown) were inside, and GAD67$^+$ postmitotic neurons surrounded them.

Thus, SFEBq culture is an efficient *in vitro* culture system for analyzing Shh signaling effects on the subpallial patterning of ESC-derived telencephalic neuroepithelial progenitors.

Temporal window for efficient subpallial differentiation in response to Shh signals

We next investigated the temporal control of subpallial differentiation, starting with the effect of Shh treatment during the early stages of SFEBq culture. SFEBq aggregates were treated with Shh (10 nM) from days 2, 3, 4, 5, or 6 until day 12, and then immunostained using pallial and subpallial markers (Fig. 2*A–E*). When Shh treatment began on day 2, 3, or 4, the pallial markers Pax6 and Tbr1 were strongly suppressed in Foxg1::venus$^+$ cells on day 12 (Fig. 2*B*,*C*, lanes 3–5). When Shh treatment began on day 5, these pallial markers were moderately suppressed (lane 6). However, they were not substantially suppressed when Shh treatment was started on day 6 (lane 7). Thus, pallial differentiation in the SFEBq aggregates was most effectively inhibited when Shh treatment was started during days 2–4.

Conversely, the subpallial markers Gsh2 and Dlx2 were effectively induced when Shh treatment was started on days 3 (Fig. 2*D*,*E*, lane 3), but not when Shh treatment began on day 6 (lane 7), compared with the control (lane 1). Therefore, this condition (starting Shh treatment on day 3) was used to analyze the temporal effects of Shh on the subpallial differentiation in the following experiments.

We next examined how many days the cells need to be exposed to Shh signals for efficient induction of subpallial differentiation and suppression of pallial differentiation. To this end, SFEBq-cultured ESCs were treated with Shh (10 nM) from day 3 for various periods. Foxg1::venus$^+$ cells were then sorted by FACS to remove nontelencephalic cells, which might affect the differentiation results, and subsequently reaggregated and cultured without Shh until day 15. In this assay, a large difference was observed between the groups sorted on day 8 and 9 (Fig. 2*F–J*), whereas those sorted on and after day 9 behaved similarly (data not shown). When treated with Shh until day 8, the reaggregates contained both Tbr1$^+$ pallial neurons and GAD67$^+$ subpallial GABAergic neurons at similar levels (Fig. 2*G*,*H*, columns 1 and 2). Cyclopamine treatment after cell sorting and reaggregation increased the percentage of Tbr1$^+$ neurons (column 3), but a substantial number of GAD67$^+$ neurons also remained (column 4). In contrast, when Shh remained in the culture until day 9, the reaggregates mostly had subpallial properties (many more GAD67$^+$ than Tbr1$^+$ cells) (Fig. 2*I*,*J*, columns 1 and 2); in this case, cyclopamine treatment after cell sorting had only a modest effect on the pallial and subpallial differentiation (columns 3 and 4). Thus, Shh-dependent subpallial specification, which is no longer sensitive to the Shh inhibitor, occurs between days 8 and 9, when cells were grown with Shh during days 3–9 in SFEBq culture.

LGE differentiation in response to Shh signals

We next examined the role of Shh signaling in the differentiation of LGE derivatives using the Nolz1 and Ctip2 markers (Fig. 2*K–*

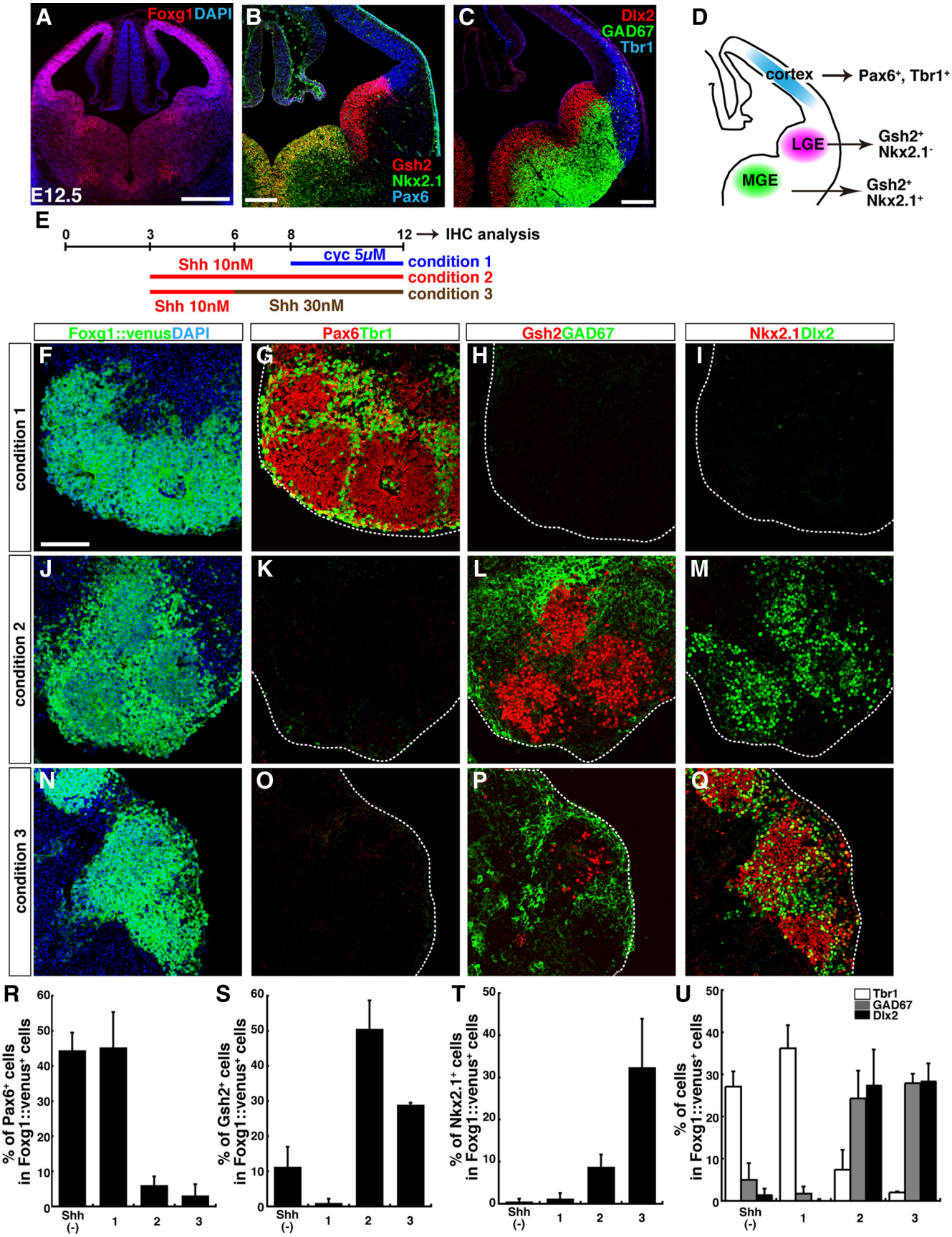

Figure 1. Selective induction of cortex-, LGE-, and MGE-type differentiation by different levels of Shh signals in SFEBq culture. ***A–C***, Coronal sections of the telencephalon of a wild-type mouse (***A***, ***B***) and a *GAD67-GFP* mouse (***C***) at E12.5. Foxg1 (***A***) is widely expressed in the telencephalon. ***B***, Region-specific neuroectodermal markers: Pax6 is expressed strongly in the cortical neuroepithelium. Gsh2 is expressed strongly in the LGE, but relatively weakly in the MGE. Nkx2.1 is mainly expressed in the MGE. ***C***, Postmitotic neuronal markers: Tbr1 is expressed (*Figure legend continues*.)

S). Nolz1 is specifically expressed in early postmitotic immature striatal neurons, which are major LGE derivatives (supplemental Fig. 2*A*, available at www.jneurosci.org as supplemental material) (Chang et al., 2004). Ctip2 also marks these cells (supplemental Fig. 2*B*, available at www.jneurosci.org as supplemental material) (Leid et al., 2004), although Ctip2 is expressed in some cortical neurons as well (note that, under the culture conditions used here, the pallial contribution was minor) (Fig. 2*J*). We focused on the effect of Shh during a several-day period after FACS cell sorting and reaggregation (Fig. 2*K*). When Shh was either not added after cell sorting, or was added at a dose of 10 nM, Nolz1$^+$/Ctip2$^+$ LGE derivatives were frequently observed. However, cyclopamine treatment starting on day 9 inhibited their expression, indicating that low levels of Shh signaling (either endogenous or exogenous) were required for proper LGE neuronal differentiation (Fig. 2*L–N*; *R*, lanes 1–3). However, high levels of Shh signaling (30 nM) inhibited LGE differentiation (Fig. 2*O*,*R*, lane 4). Furthermore, treatment with the potent Hedgehog agonist SAG at 100 nM also strongly inhibited LGE differentiation (Fig. 2*P*,*R*, lane 5), but induced the MGE-derivative markers SOM and *Lhx6* (Lavdas et al., 1999; Du et al., 2008), instead (Fig. 2*Q*,*S*, lane 5).

Together, these observations show that the differentiation of LGE derivatives (double-positive for Nolz1 and Citp2) from ESCs was preferentially induced when cells were treated with a moderate dose of Shh (10 nM) from day 3, sorted and reaggregated on day 9, and subsequently cultured in the presence of endogenous or exogenous Shh (10 nM).

Efficient *in vitro* striatal precursor differentiation from ESC-derived FACS-purified Foxg1$^+$ progenitors

In the embryonic LGE, multiple levels of neuronal differentiation and maturation are identified with molecular markers (Fig. 3*A–F*). At E15.5, Gsh2 is expressed primarily in the apical-most part of the LGE ventricular zone, whereas Dlx2 is expressed both in the ventricular and subventricular zones, and subsets of maturing neurons (Fig. 3*A*,*B*) (Long et al., 2009b). Nolz1 and Ctip2 are expressed in both the subventricular zone and the maturing neurons of the striatum (Fig. 3*A*,*C*,*D*). However, Foxp1 and Ikaros are expressed in the striatum (Fig. 3*E*; supplemental Fig. 3*A*, available at www.jneurosci.org as supplemental material) (Ferland et al., 2003; Agoston et al., 2007; Long et al., 2009b).

With these facts in mind, we performed a time course analysis of the neuronal differentiation of LGE progenitors generated in SFEBq culture at the medium dose of Shh (10 nM) from days 3–9 (Fig. 3*G–S*). Foxg1::venus$^+$ cells were FACS-purified, reaggregated, and further cultured without Shh until day 18. The Nolz1$^+$/Ctip2$^+$ population increased substantially during days 12–15, but no subsequent increase was seen during days 15–18 (Fig. 3*J–M*). In contrast, the population of cells positive for Foxp1$^+$/Ctip2$^+$, which are more advanced markers of striatal neurons, continued to increase during days 15–18 (Fig. 3*N–Q*). Consistent with this, DARPP32, a marker for medium-sized spiny neurons (main projection neurons of the striatum) (Ouimet et al., 1998) and Ikaros were also detected preferentially on day 18 (Fig. 3*R*,*S*; supplemental Fig. 3*B*,*C*, available at www.jneurosci.org as supplemental material).

These findings demonstrate that SFEBq-cultured ESCs treated with a properly timed, moderate Shh dose differentiate into LGE derivatives (striatal neurons) after molecularly defined steps consistent with temporal patterns of gene expression *in vivo*.

ESC-derived striatal precursors mature into medium-sized spiny neurons *in vitro* and *in vivo*

We next analyzed the generation of mature striatal neurons in long-term culture (Fig. 4*A–I*). Cultured cells were sorted and reaggregated in medium including Shh (10 nM). On day 13, cells were dissociated and further cultured until day 35 in the presence of rat glial conditioned medium without Shh. Under these conditions, ~50% of the ESC-derived Foxg1::venus$^+$ telencephalic neurons expressed DARPP32 (Fig. 4*B*,*D*). In contrast, few DARPP32$^+$ neurons were found when Shh signaling was either blocked (with cyclopamine), or was excessively activated (with SAG), during the postsorting reaggregation culture (Fig. 4*A*,*D*) (consistent with the Nolz1/Ctip2 induction data in Fig. 2*R*). As in the embryonic striatum, the ESC-derived DARPP32$^+$ neurons expressed GAD67 (Fig. 4*C*,*D*), which is consistent with the medium-sized spiny neurons being GABAergic (Mink, 2008). They also expressed Ctip2 (Fig. 4*E*,*F*) (79% in DARPP32$^+$/Foxg1::venus$^+$ neurons). Furthermore, like authentic striatal neurons, their dendrites had numerous spines (Fig. 4*G–I*). Thus, SFEBq culture of ESCs with a moderate Shh dose (LGE differentiation culture), combined with FACS sorting on day 9, is an efficient method for generating precursors for striatal projection neurons.

We next tested whether these ESC-derived precursors would differentiate into striatal neurons *in vivo* (Fig. 4*J–U*). After LGE differentiation culture, Foxg1::venus$^+$ ESCs were purified by FACS on day 9 and reaggregated in suspension culture in the presence of 10 nM Shh until day 13. The cells were then dissociated and injected into postnatal day 2 (P2) mouse striatum ($1–2 \times 10^6$ cells/injection). Three weeks after the transplantation, Foxg1::venus$^+$ neurons were found in the host striatum (the frequency of surviving neurons per injected neurons was 4.7%). Almost all the surviving Foxg1::venus$^+$ neurons in the striatum coexpressed DARPP32 (14 experiments) and showed a morphology typical of medium-sized spiny neurons (Fig. 4*K–N*). The Foxg1::venus$^+$ neurons did not coexpress the cortical-plate neuron marker Tbr1 or the interneuron markers SOM or PV. In contrast, when injected into the cortex, only 32% of the surviving Foxg1::venus$^+$ neurons expressed DARPP32, suggesting that a significant local environmental selection may have contributed to the highly specific integration of ESC-derived DARPP32$^+$ neurons in the striatum. As a negative control, we transplanted Foxg1::venus$^+$ cells that have been cultured under cortex differentiation conditions (5 μM cyclopamine during days 8–15) into P2 mouse striatum; in this case, the grafted neurons in the striatum did not express DARPP32 (five experiments), and 93% of the surviving neurons were Tbr1$^+$ (supplemental Fig. 4*A–C*, available at www.jneurosci.org as supplemental material). This

←

(*Figure legend continued*.) in the cortex. Dlx2 and GAD67 are expressed widely in the subpallial region. ***D***, Schematic of the subregions of the developing telencephalon in a coronal section. ***E***, Differentiation culture for region-specific telencephalic cells from ESCs. ***F–I***, Serial sections of SFEBq-cultured *Foxg1::venus* ES cell aggregates on day 12. ESCs were cultured in condition 1. Cyclopamine (5 μM) was added on day 8. ***J–M***, Serial sections of cell aggregates cultured in condition 2. Shh (10 nM) was added on day 3. ***N–Q***, Serial sections of cell aggregates cultured in condition 3. Shh was added on days 3 (10 nM) and 6 (30 nM). Sections were immunostained for GFP (***F***, ***J***, ***N***), Pax6/Tbr1 (***G***, ***K***, ***O***), Gsh2/GAD67 (***H***, ***L***, ***P***), or Nkx2.1/Dlx2 (***I***, ***M***, ***Q***), and counterstained with DAPI (4′,6′-diamidino-2-phenylindole). The dotted lines outline cell aggregates (***G–I***, ***K–M***, ***O–Q***). ***R–U***, Percentage of cells positive for the mitotic markers; Pax6 (***R***), Gsh2 (***S***), or Nkx2.1 (***T***), and for the postmitotic markers; Tbr1, GAD67, or Dlx2 (***U***). Shh (−), Culture without exogenous Shh or cyclopamine. Error bars indicate SEM. Scale bars: ***A***, 500 μm; ***B***, ***C***, 200 μm; ***F–Q***, 100 μm.

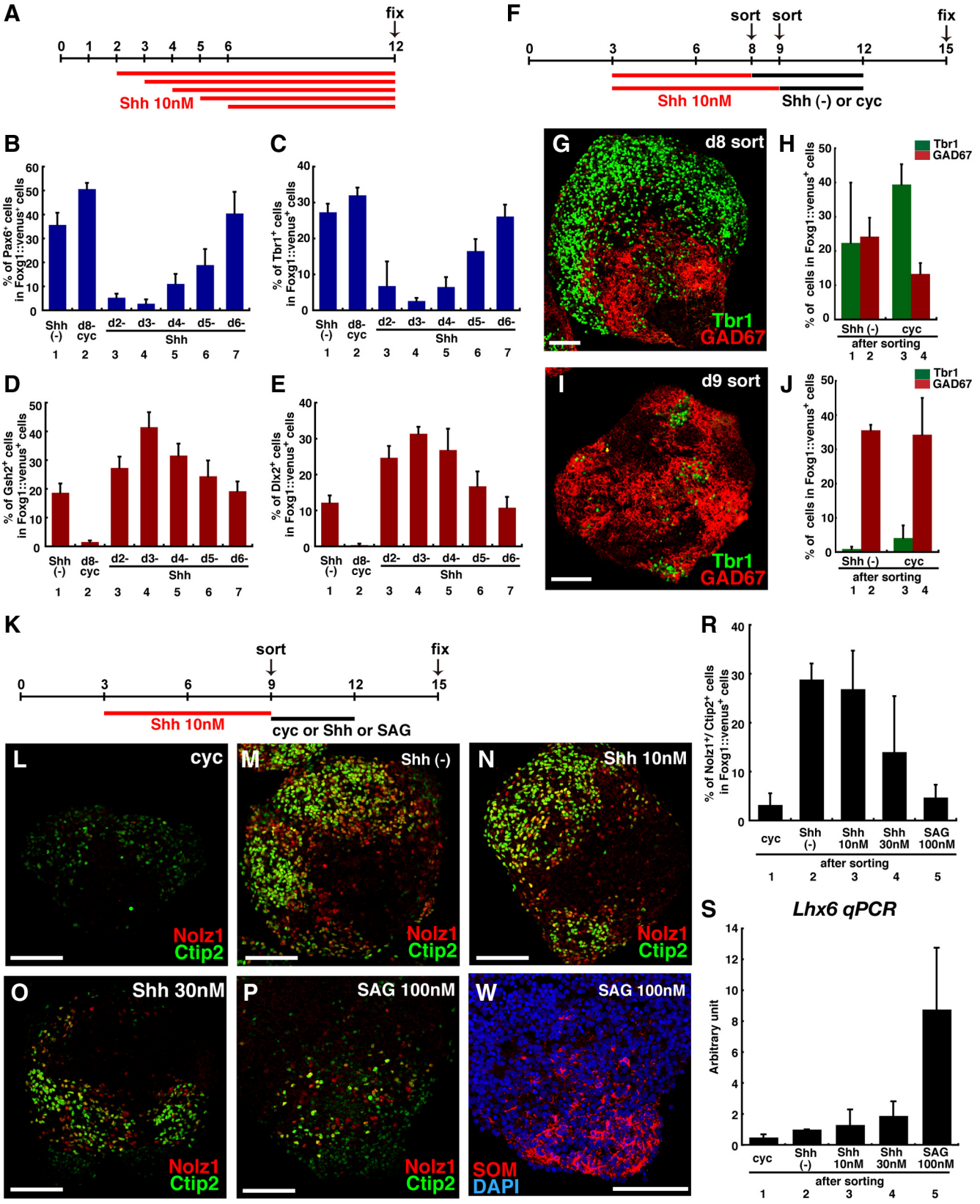

Figure 2. Temporal window for efficient subpallial differentiation in response to Shh signals. ***A***, Temporal differences in Shh's effect on ES cell culture. ***B–E***, Percentage of Foxg1::venus $^{+}$ cells treated with cyclopamine (5 μM) from day 8, or with Shh (10 nM) from day 2, 3, 4, 5, or 6 that were positive for Pax6 (***B***), Tbr1 (***C***), Gsh2 (***D***), or Dlx2 (***E***). ***F***, FACS sorting at different time points. Shh (10 nM) was added on day 3. ***G***, ***I***, Tbr1 and GAD67 expression in Foxg1::venus $^{+}$ cells sorted on day 8 (***G***) or day 9 (***I***) and subsequently cultured without cyclopamine. ***H***, ***J***, Percentage of Foxg1::venus $^{+}$ cells sorted on day 8 (***H***) or day 9 (***J***) that were positive for Tbr1 $^{+}$ or GAD67 $^{+}$. Shh (−), Cells treated without Shh or cyclopamine after sorting; cyc, cells treated with cyclopamine (1 μM) after sorting. ***K***, LGE induction experiments, examining the effect of Shh signaling after sorting. Shh (10 nM) was added to the cell culture on day 3. Foxg1::venus $^{+}$ cells were sorted and reaggregated on day 9. ***L–P***, LGE markers (Nolz1/Ctip2) expressed in Foxg1::venus $^{+}$ reaggregates treated after sorting with 1 μM cyclopamine (***L***), nothing (***M***), 10 nM Shh (***N***), 30 nM Shh (***O***), or 100 nM SAG (***P***). ***Q***, SOM in Foxg1::venus $^{+}$ reaggregates treated with 100 nM SAG after sorting. ***R***, Percentage of Nolz1/Ctip2 double-labeled cells. ***S***, qPCR analysis for the *Lhx6* (*Figure legend continues.*)

suggests that the lineage of Foxg1::venus$^+$ cells was already mostly restricted before grafting by the differentiation conditions in the SFEBq cultures.

A previous study using human ESCs also reported that ESC-derived neural precursors cultured with Shh could produce some striatal neurons when grafted into the quinolinate-lesioned striatum of immunosuppressed rats (Aubry et al., 2008). However, transplantation of these cells frequently caused large tumors to form. In contrast, we did not observe any tumorigenesis in transplants of ESC-derived striatal neurons ($n = 14$). As cells were not sorted and purified before being transplanted in the study by Aubry et al. (2008), we tested whether the FACS sorting and purifying of Foxg1::venus$^+$ cells eliminated tumor formation in our case.

We injected ESCs that had been cultured in LGE differentiation conditions, but not sorted by FACS, into the striatum. In this case, tumor-like overgrowths were observed in the host brain (100%; $n = 5$; 3 weeks after transplantation). These collections of cells contained Sox1$^+$ neural progenitors, Tuj1$^+$ neurons, and GFAP$^+$ glia-like cells, but not Oct3/4$^+$ germinal cells (supplemental Fig. 4*D–J*, available at www.jneurosci.org as supplemental material). These results suggest that these lesions represented neural overgrowth rather than teratoma. These findings indicate that FACS purification of telencephalic cells is important for the generation of striatal grafts that do not contain poorly differentiated cells capable of forming neurogenic tumors.

We next analyzed the differentiation and integration of ESC-derived striatal neurons. The major projections of striatal medium-sized spiny neurons point toward the globus pallidus and the substantia nigra pars reticulata (Bolam et al., 2000) (these axons can be detected by immunostaining with DARPP32) (Fig. 4*J*). Immunostaining of the host brain showed that Foxg1::venus$^+$ axons from transplanted striatal neurons formed fascicles running parallel to the corticofugal fibers in the striatum (Fig. 4*O*,*P*). These venus$^+$ axons ipsilaterally reached the globus pallidus (Fig. 4*Q*) (seen as numerous branches), the cerebral peduncle (Fig. 4*R*,*S*), and the subthalamic/nigral region (Fig. 4*T*,*U*) (data not shown), and thus followed the pathway of the endogenous DARPP32$^+$ striatal axons. No substantial Foxg1::venus$^+$ cells or projection was seen entering the cortex or extending outside of the extrapyramidal (striatopallidal/striatonigral) tract.

Together, these findings show that ESC-derived striatal neurons have similar molecular, morphological, and hodological properties with endogenous medium-sized spiny neurons.

FGF signals modulate the fate of SAG-induced ventral subpallial cells

Although a moderate, continuous Shh dose induced LGE differentiation in SFEBq culture, LGE differentiation was inhibited by high Hedgehog signaling levels (100 nM SAG) after FACS sorting, as shown in Figure 2*K–S*. The SAG-treated cells, instead, expressed *Lhx6*, a marker for MGE-derived interneurons.

For a more detailed study of the effect of high Hh signals on the subregional specification of ESC-derived telencephalic cells, SFEBq-cultured ESCs were treated with SAG during days 3–6 (3 nM) and 6–8 (10 nM), and again on day 8 after FACS sorting (100 nM) (Fig. 5*A*). These SAG concentrations during the period before FACS sorting did not inhibit the later telencephalic differentiation of the cells, as measured by Foxg1::venus expression (supplemental Fig. 1*H–N*, available at www.jneurosci.org as supplemental material). The expression of Nkx2.1 was dependent on high-dose SAG treatment during days 8–12, and few Nkx2.1$^+$ cells were observed in the absence of SAG (Fig. 5*B–D*). Reaggregates treated with high-dose SAG contained a number of SOM$^+$/GAD67$^+$ neurons, reminiscent of subpallium-derived interneurons *in vivo* (Fig. 5*E*).

We therefore investigated the ability of the cells to migrate in a coculture assay with embryonic (E13.5) forebrain slices. The reaggregates were cultured in the presence of 100 nM SAG until day 15, and placed en bloc on the forebrain slice at the subventricular zone near the interganglionic sulcus (Fig. 5*F–K*). Three days later, Foxg1::venus$^+$ cells were seen migrating out of the reaggregate through the LGE and into the cortex (Fig. 5*G*,*I–K*). Some cells were even found in the dorsal neocortex (Fig. 5*K*), indicating that ESC-derived neurons induced by high SAG had strong migratory ability, as is also true for MGE/CGE-derived cortical interneurons (Anderson et al., 1997, 2001; Wichterle et al., 1999; Yozu et al., 2005). In contrast, when reaggregates were cultured in the absence of Hh signaling after sorting and were placed on the same position of the forebrain slice, the Foxg1::venus$^+$ cells rarely migrated into the cortex (Fig. 5*H*), indicating that their ability to migrate was affected by Hh signaling after sorting.

A dissociation culture of the SAG-treated reaggregates produced almost exclusively GAD67$^+$ GABAergic neurons (Fig. 5*L*) (data not shown), including those expressing the cortical interneuron markers SOM, NPY, and PV (Fig. 5*L–N*). This expression profile was dependent on SAG treatment after sorting (Fig. 5*O*).

We next analyzed the subregional nature of cells in the SAG-treated reaggregates. Cortical interneurons originate in both the MGE and the CGE; these two ganglionic eminences are demarcated by molecular markers. For instance, Nkx2.1 is expressed in the MGE (Fig. 6*A*,*B*) (MGE-derived cortical interneurons extinguish Nkx2.1 expression as they differentiate and migrate). However, Nkx2.1 is not expressed in the CGE at all (Fig. 6*A*,*C*). In contrast, the CGE, but not the MGE, strongly expresses CoupTFII (Fig. 6*A–D*) (in the subpallium, CoupTFII is more preferentially expressed in the caudal domain than CoupTFI, which is expressed also in part of the LGE and the MGE) (Tripodi et al., 2004; Kanatani et al., 2008; Long et al., 2009a). The SAG-treated reaggregates contained a substantial number of Nkx2.1$^+$ cells and CoupTFII$^+$ cells (Fig. 6*E*,*F*), with a minor double-positive population, suggesting that both MGE- and CGE-type cells were present in these reaggregates.

We next attempted to generate a larger percentage of MGE-type cells. In the embryonic subpallium, the MGE is located rostral to the CGE along the neural axis. Previous studies have shown that the rostral-caudal regional specification of the pallium is regulated by Fgf signals. Loss- and gain-of-function analyses have demonstrated that Fgf8, which is strongly expressed in the commissural plate (located at the rostral end of telencephalon), promotes rostral specification of the cortex. *Fgf8* mutant mice (hypomorphic or with a telencephalon-specific conditional null allele) have a reduced size of the rostral cortex, and have a rostral expansion of CoupTFI expression, which positively regulates the caudal cortical fate (Garel et al., 2003; Storm et al., 2006). Furthermore, augmenting the endogenous Fgf8 signal shifts rostral-caudal boundaries of the cortical areas caudally, whereas

←

(*Figure legend continued.*) for the *Lhx6* expression in Foxg1::venus$^+$ reaggregates on day 15. Each lane indicates the condition after sorting. Error bars indicate SEM. Scale bars: ***G***, ***I***, ***L–Q***, 100 μm.

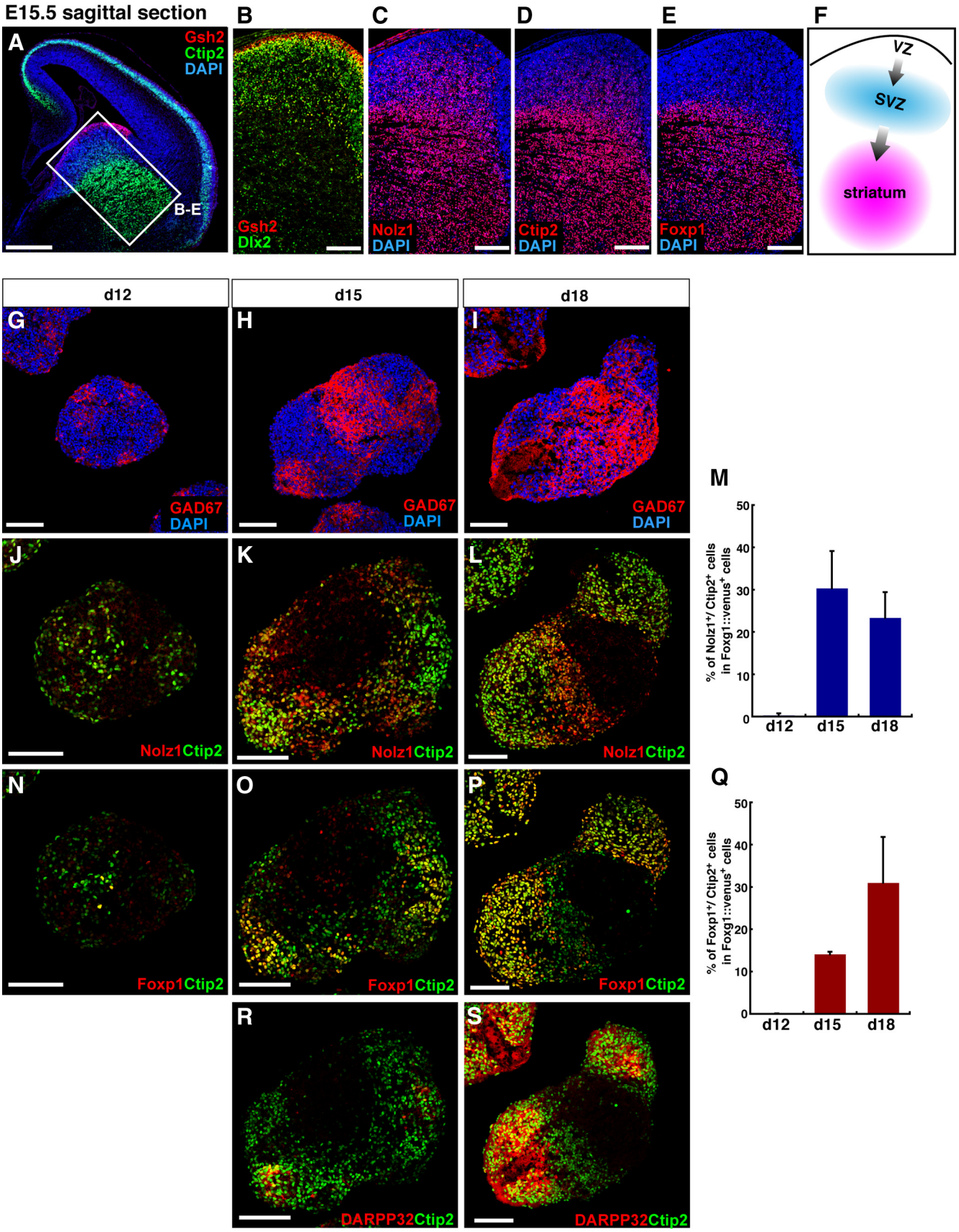

Figure 3. Efficient *in vitro* striatal precursor differentiation from ESC-derived FACS-purified Foxg1^{+} progenitors. ***A–E***, Sagittal sections of an E15.5 mouse telencephalon, immunostained with Gsh2 (***A***, ***B***), Ctip2 (***A***, ***D***), Dlx2 (***B***), Nolz1 (***C***), and Foxp1 (***E***), and counterstained with DAPI. ***F***, Schematic of the migration of LGE-derived striatal neurons. ***G–S***, Time course of LGE-type differentiation. ES cell aggregates were treated with 10 nM Shh during days 3–9, sorted and reaggregated on day 9, and cultured without Shh after sorting. Foxg1::venus^{+} cell aggregates were fixed on day 12 (***G***, ***J***, ***N***), day 15 (***H***, ***K***, ***O***, ***R***), and day 18 (***I***, ***L***, ***P***, ***S***). Sections were immunostained with GAD67 (***G–I***), Nolz1/Ctip2 (***J–L***), Foxp1/Ctip2 (***N–P***), or DARPP32/Ctip2 (***R***, ***S***). (*Figure legend continues*.)

attenuating the Fgf8 signaling shifts these boundaries rostrally (Fukuchi-Shimogori and Grove, 2001). Consistent with this, our previous *in vitro* ESC study showed that SFEBq-induced pallial neural tissues are directed to acquire a rostral identity in the presence of Fgf8 signaling and a caudal identity in its absence (Eiraku et al., 2008). In addition, a previous genetic study (Storm et al., 2006) demonstrated that MGE expression of Nkx2.1 is severely reduced in the *Fgf8* mutant mice. Based on these previous findings, here we tested whether we could coax SAG-treated reaggregates to differentiate preferentially into Nkx2.1$^+$ MGE cells by manipulating Fgf8 signals after sorting (Fig. 6*E–J*).

When SAG-treated reaggregates were cultured in the presence of Fgf8 during days 8–12, the percentage of Nkx2.1$^+$ cells substantially increased, whereas that of CoupTFII$^+$ cells decreased moderately (Fig. 6*G*), resulting in a high ratio of Nkx2.1$^+$ to CoupTFII$^+$ cells in the Fgf8-treated cultures (Fig. 6*I*, lane 3). Conversely, when Fgf signaling was blocked by the FgfR3c receptobody, which binds Fgf8b with high affinity (MacArthur et al., 1995), or by the FgfR inhibitor PD173074 (Skaper et al., 2000), the CoupTFII$^+$ population predominated over the Nkx2.1$^+$ population (Fig. 6*I*, lanes 4, 5). The total GABAergic neuronal differentiation, however, was not substantially affected by these Fgf inhibitors (supplemental Fig. 5*B*, available at www.jneurosci.org as supplemental material). Furthermore, the MGE-derivative marker *Lhx6* was increased by Fgf8 treatment and reduced by the inhibition of Fgf signals (Fig. 6*J*, lanes 3–5). These findings indicate that the specification of MGE-type Nkx2.1$^+$ cells, which are located in the ventral and rostral subpallium *in vivo*, is dependent on Fgf8- or Fgf-related signals in SFEBq culture in the presence of high Hh signaling.

A recent genetic study provided evidence that Fgf8 and Fgf15/19 (which are homologs in mouse and human) have opposite roles in the rostral-caudal patterning of the mouse pallium (Borello et al., 2008). Fgf8 represses the expression of the caudal cortical marker CoupTFI, whereas Fgf15 promotes its expression. We therefore examined the effect of the Fgf15/19 signals on SAG-treated reaggregates. Interestingly, in contrast to Fgf8 treatment, treatment with Fgf15/19 promoted CoupTFII expression at the expense of Nkx2.1 expression (Fig. 6*H*,*I*, lane 6), whereas the Fgf15/19 treatment did not affect total GABAergic neuronal differentiation (supplemental Fig. 5*A*,*B*, available at www.jneurosci.org as supplemental material). In addition, unlike Fgf8, Fgf15/19 inhibited the expression of *Lhx6*, a gene marker for MGE-derived neurons (Fig. 6*J*, lane 6). When SAG-treated reaggregates were exposed simultaneously to both Fgf8 and Fgf15/19, Nkx2.1 was strongly induced and at the expense of CoupTFII, much as in cultures treated with Fgf8 alone (Fig. 6*I*, lane 7).

We next examined whether the Fgf15/19 treatment affected the migratory ability of the cells in a coculture assay similar to that shown in Figure 5*F–K*. A Foxg1::venus$^+$ reaggregate treated with SAG and Fgf15/19 after sorting (CGE induction conditions) was placed on the forebrain slice at the subventricular zone of the CGE. In those conditions, Foxg1::venus$^+$ cells actively migrated out of the reaggregate toward the cortex (Fig. 6*K*). Similarly to the cells treated with SAG alone (Fig. 5*G*), some Foxg1::venus$^+$ cells cultured in the CGE induction conditions reached the marginal zone of the dorsal neocortex (Fig. 6*L*,*M*) where immature migrating interneurons are often observed in neonatal mice (Anderson et al., 1997). In addition, we observed that some of the migratory Foxg1::venus$^+$ cells coexpressed calbindin, a marker expressed in some of the migrating CGE-derived interneurons *in vivo* (Fig. 6*N*) (Kanatani et al., 2008). A similar efficient migration was observed when a reaggregate treated with SAG and Fgf8 (MGE induction conditions) was placed on the MGE region of the forebrain slice (data not shown).

Several *in vivo* studies showed that a majority of MGE-derived cortical interneurons are positive for SOM or PV, whereas the CGE-derived cortical interneurons preferentially express CAR and/or vasointestinal peptide (VIP) (Xu et al., 2004; Butt et al., 2005; Wonders and Anderson, 2006). We next analyzed whether Fgf8 or Fgf15/19 treatment altered the expression profile of interneuron subtype markers (Fig. 6*O–Q*). In dissociation culture, Foxg1::venus$^+$ cells cultured in the MGE induction conditions displayed a similar expression profile to those treated with SAG alone (Fig. 6*Q*, blue columns; compare with Fig. 5*O*, red columns). In contrast, the CGE induction conditions increased CAR$^+$ cells and decreased SOM$^+$, NPY$^+$, and PV$^+$ cells (Fig. 6*O–Q*), a tendency consistent with the *in vivo* observation. VIP$^+$ cells were not observed in the ESC-derived subpallial cells cultured under any conditions tested in this study, suggesting that environmental factors are required to induce their differentiation. These results indicate that distinct Fgf signals also have differential effects on the interneuron subtype specification.

Together, these findings demonstrate that the subregional specification of ESC-derived subpallial tissues can be controlled in a temporally restricted manner by two separate signaling systems *in vitro*: graded Hh signaling and antagonistic Fgf8 versus Fgf15/19 signaling.

Discussion

Temporal control and flexibility of the subregional fate specification of ESC-derived telencephalic tissues

ESC-derived telencephalic progenitors in SFEBq culture differentially generated neural cells expressing pallial, dorsal and ventral subpallial markers with Shh treatment in a dose-dependent manner (Fig. 1). Interestingly, efficient induction of subpallial differentiation at the cost of pallial differentiation was critically dependent on the timing of exposure to Shh signaling: Shh exposure starting at an early phase of SFEBq culture (e.g., day 3) induced efficient subpallial differentiation, whereas late exposure (Shh treatment starting on days 5 or 6) failed to suppress pallial differentiation (Fig. 2*A–E*). This temporal dependence suggests that Shh signals contribute to the formation of a prepattern in early neuroectodermal progenitors with a ventrally directed bias (subpallial direction) even before the general telencephalic marker Foxg1 is first detected on day 6. This idea is consistent with a previous *in vivo* study using constitutively active Smo (Smoothened)-expressing virus (Rallu et al., 2002a) and also consistent with the early specification study of the chick subpallium (Gunhaga et al., 2000).

However, the detailed mode and timing of the action of Shh for subpallial specification *in vivo* has remained mostly elusive (Kohtz et al., 1998; Rallu et al., 2002b; Fuccillo et al., 2006; Lupo et al., 2006; Hébert and Fishell, 2008; Xu et al., 2010). In our study, exogenous Shh signals (starting on day 3) needed to be present continuously until day 9 to selectively commit ESC-derived telencephalic progenitors to a subpallial fate (Fig. 2*I*,*J*). When treated with Shh only during days 3–8, a substantial portion of SFEBq-induced telencephalic cells still differentiated into

←

(*Figure legend continued.*) ***M***, ***Q***, Percentage of Nolz1/Ctip2 (***M***) and Foxp1/Ctip2 (***Q***) double-labeled cells. Error bars indicate SEM. Scale bars: ***A***, 500 μm; ***B–E***, 200 μm; ***G–L***, ***N–P***, ***R***, ***S***, 100 μm.

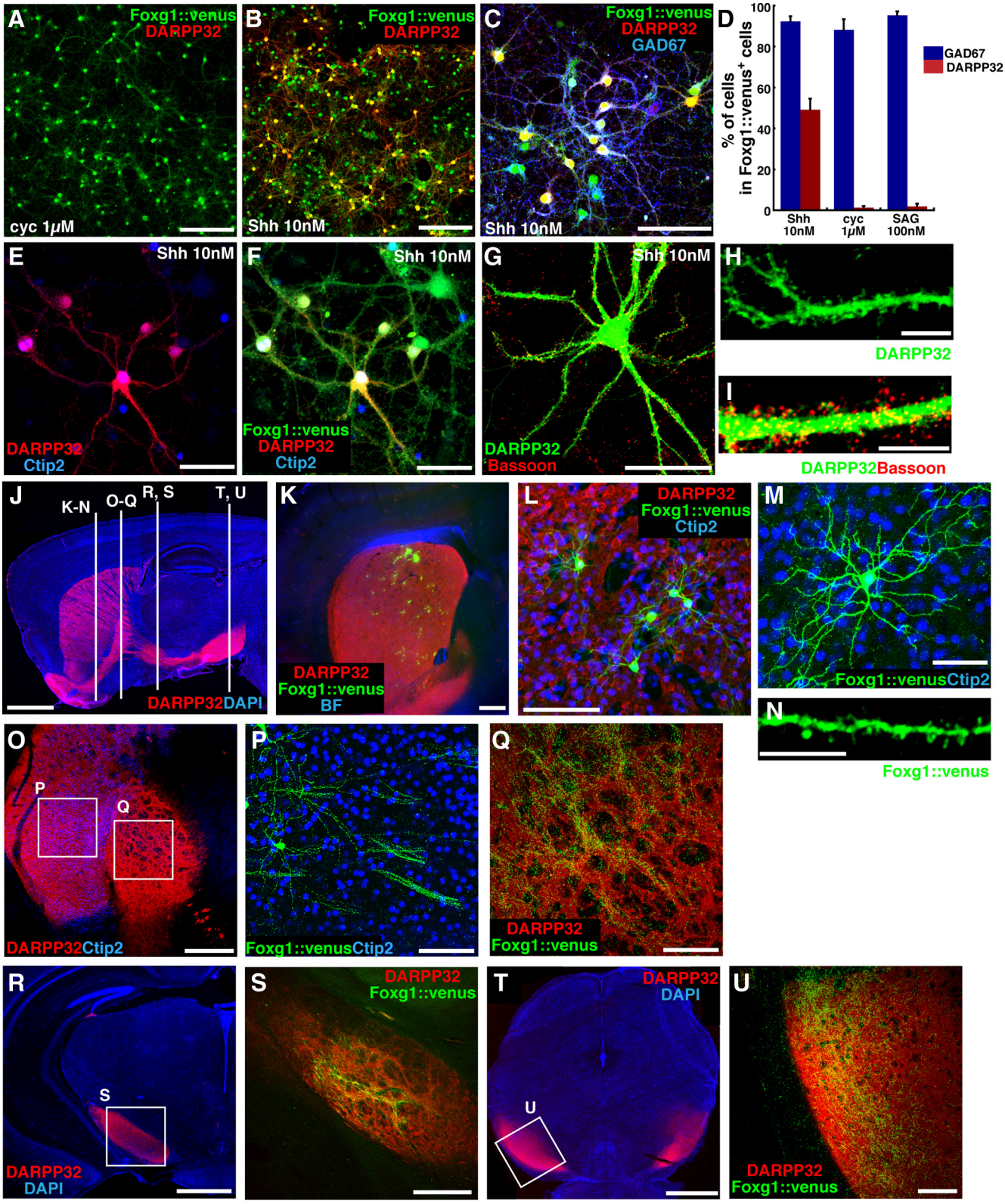

Figure 4. ESC-derived striatal precursors mature into medium-sized spiny neurons *in vitro* and *in vivo*. ***A–I***, Adhesion culture of LGE-type Foxg1::venus $^{+}$ cells. ESCs were treated with Shh (10 nM) during days 3–9, sorted and reaggregated on day 9, redissociated and replated on day 13, and fixed on day 35. ***A–C***, Shh signaling effect on DARPP32 after sorting. ***A***, Cyclopamine treatment (1 μM; days 9–13). ***B***, ***C***, Shh treatment (10 nM; days 9–13). ***D***, Percentage of GAD67 $^{+}$ and DARPP32 $^{+}$ cells. Each lane indicates the condition after sorting. Error bars indicate SEM. ***E–I***, Foxg1::venus $^{+}$ cells treated with 10 nM Shh after sorting (days 9–13), immunostained with DARPP32 (***E–I***), Ctip2 (***E***, ***F***), GFP (***F***), and Bassoon (***I***; marker for presynaptic terminal). ***H***, ***I***, Magnified view of numerous spines on dendrites of a DARPP32 $^{+}$ neuron. ***J***, Trajectory of striatonigral axon fibers in a sagittal section of the adult mouse brain, immunostained with DARPP32. ***K***, LGE-type Foxg1::venus $^{+}$ cells integrated in the striatum. ***L***, Magnified view of grafted Foxg1::venus $^{+}$ cells. ***M***, Morphology of a grafted Foxg1::venus $^{+}$ cell. ***N***, Numerous spines were observed on a dendrite of a grafted Foxg1::venus $^{+}$ cell. ***O–U***, Grafted Foxg1::venus $^{+}$ cells extended axons to the globus pallidus (***O–Q***), the cerebral peduncle (***R***, ***S***), and the substantia nigra (***T***, ***U***). ***P***, ***Q***, ***S***, and ***U*** are high-magnification views of the corresponding squares in ***O***, ***R***, and ***T***. Scale bars: ***A***, ***B***, 200 μm; ***C***, ***P***, ***L***, ***Q***, ***U***, 100 μm; ***E–G***, ***M***, 50 μm; ***H***, ***I***, ***N***, 10 μm; ***J***, 2 mm; ***K***, ***O***, 500 μm; ***R***, ***T***, 1 mm; ***S***, 300 μm.

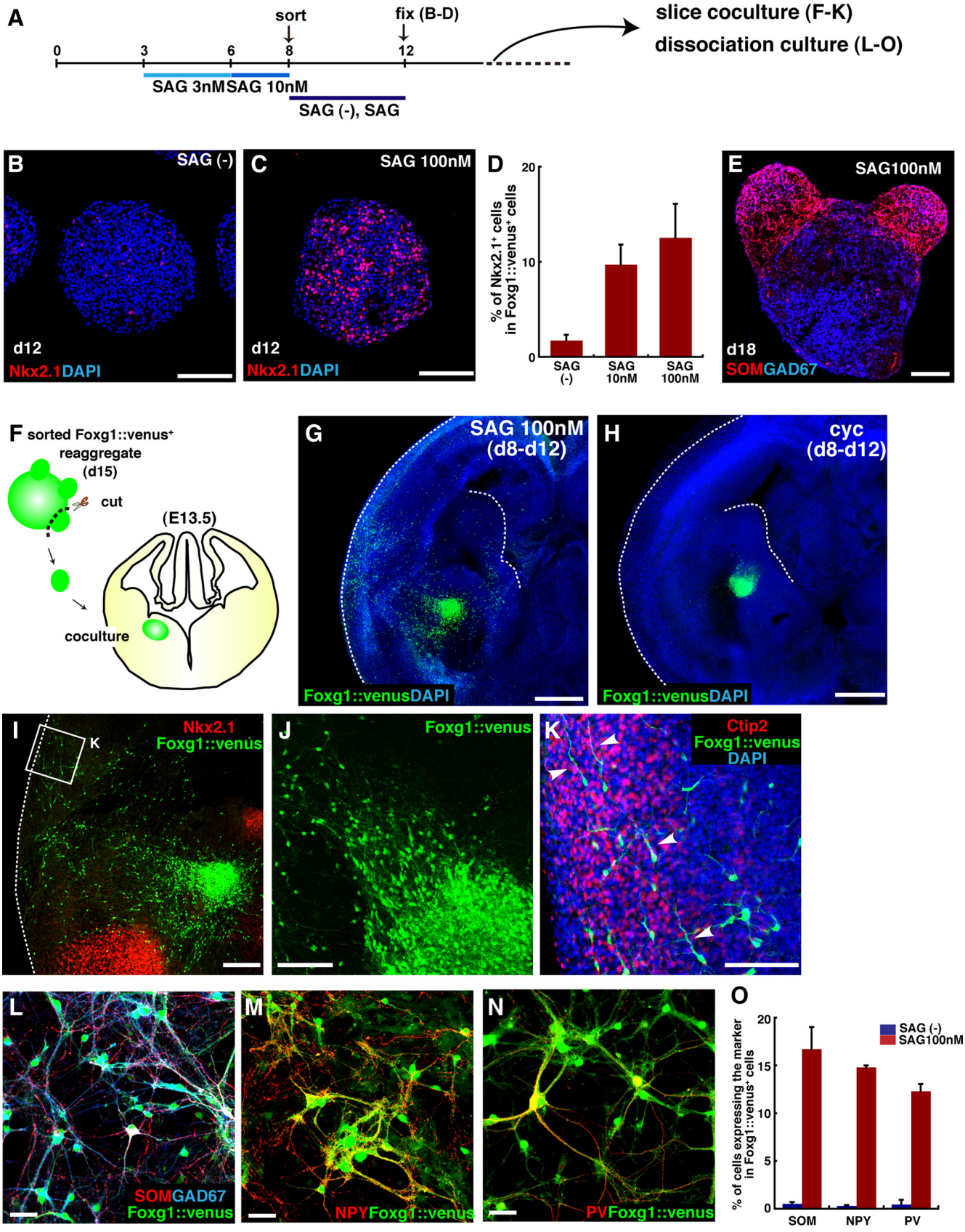

Figure 5. MGE specification from ESC-derived FACS-purified Foxg1 $^{+}$ progenitors in response to high dose of SAG. ***A***, MGE induction experiments. SAG was added on days 3 (3 nM) and 6 (10 nM). Foxg1::venus $^{+}$ cells were sorted on day 8. ***B***, ***C***, Hh signaling effect on Nkx2.1 expression in cells with no treatment (***B***) and with SAG treatment (100 nM) (***C***) after sorting. ***D***, Percentage of Nkx2.1 $^{+}$ cells in Foxg1::venus $^{+}$ cells. Each lane indicates the conditions after sorting. ***E***, SAG-treated Foxg1::venus $^{+}$ cell reaggregate, immunostained on day 18. SOM $^{+}$ neurons protruded from the body of the reaggregates. ***F***, Schematic of the slice coculture for a migration assay of Foxg1::venus $^{+}$ cells. ***G–J***, Immunostaining of a slice cocultured with Foxg1::venus $^{+}$ cell mass. Active migration toward the cortex was observed in Foxg1::venus $^{+}$ cells treated with 100 nM SAG (***G***), but not in those treated with 1 μM cyclopamine (***H***). The dotted lines in ***G*** and ***H*** (*Figure legend continues.*)

a pallial fate after FACS purification (Fig. 2*G*,*H*). The relationship between the duration and strength of Shh signaling for *in vitro* subpallial differentiation is somewhat complicated. For instance, SFEBq-induced telencephalic cells cultured without a Hh agonist or antagonist (meaning that they were only exposed to low endogenous Hh signaling) during days 3–9 could be partially steered to differentiate into subpallial (GABAergic) neurons when they were treated with 100 nM SAG after FACS sorting (supplemental Fig. 2*C*,*D*, condition 2, available at www.jneurosci.org as supplemental material). Interestingly, when the endogenous Shh signaling was actively blocked by cyclopamine only for 1 d (during days 8–9), they did not substantially differentiate into GABAergic neurons, even in the presence of high-dose SAG in subsequent culture (supplemental Fig. 2*C*,*D*, condition 4, available at www.jneurosci.org as supplemental material).

In this study, the Shh agonist, SAG, which is much less expensive than recombinant Shh proteins, worked reproducibly and robustly to control region-specific differentiation without any obvious cell toxicity or adverse effects, even at a high concentration (100 nM). We previously reported that purmorphamine (which targets the Hh receptor Smoothened) effectively ventralizes diencephalic progenitors in a modified SFEBq culture (Wataya et al., 2008). However, unlike Shh treatment, purmorphamine reduces SFEBq aggregate size, suggesting a negative side effect on cell proliferation.

Role of FGF signaling in the subregional specification of telencephalic progenitors

The region of CGE is a distinct tissue, containing progenitors that contribute to both cortical and subcortical telencephalic neurons (Nery et al., 2002), whereas its specification has mostly remained elusive. Our present study offers some hints regarding the mechanism for CGE specification. Two distinct Fgf signals have differential effects on the Nkx2.1 and CoupTFII induction in ESC-derived, SAG-treated subpallial cells. Fgf8 treatment increased the percentage of Nkx2.1$^+$ cells at the cost of CoupTFII$^+$ cells, whereas Fgf15/19 treatment had the opposite effect. These findings have some parallels with the previous reports on the roles of these Fgfs in pallial patterning along the rostral-caudal axis (Borello et al., 2008). They showed that, in the embryonic pallium, Fgf8 inhibits expression of the caudal cortical marker CoupTFI, whereas Fgf15/19 promotes it. Since the Nkx2.1$^+$ MGE domain is located rostral to the CoupTFII$^+$ CGE domain in the embryonic subpallium, it appears that the antagonistic signal set of Fgf8 and Fgf15/19 is capable of controlling the rostral-caudal specification in both pallial and subpallial tissues. Furthermore, Fgf15, unlike Fgf8, is expressed in the CGE, where it could promote CGE development [additional files 1 and 2 in the study by Borello et al. (2008)].

Why, then, did the SAG-treated ESC-derived telencephalic cells differentiate into CGE tissues in the absence of exogenous Fgf signals (Fig. 6*F*,*I*, lane 2)? Interestingly, our preliminary qPCR analysis showed that strong Hh signaling (>100 nM SAG) in the ESC-derived neural precursors tended to increase endogenous *Fgf15*, whereas the expression of endogenous *Fgf8* was suppressed (supplemental Fig. 5*D–F*, available at www.jneurosci.org as supplemental material). Thus, high Hh signaling not only causes strong ventralization in the SFEBq-cultured telencephalic cells but also creates a relative Fgf15-high/Fgf8-low bias in culture (illustrated in supplemental Fig. 5*J*, available at www.jneurosci.org as supplemental material). This idea agrees with the observation that the added exogenous Fgf8 was necessary for the efficient rostral-ventral differentiation marked by Nkx2.1. The positive regulation of *Fgf15* expression by Shh has been also reported in the previous *in vivo* mouse studies of the forebrain and midbrain development (Ishibashi and McMahon, 2002; Borello et al., 2008).

At the transcriptional control level, no strong mutual interactions between *Fgf8* and *Fgf15* expression were observed in SFEBq culture. Fgf15/19 treatment did not alter the expression of *Fgf8* (supplemental Fig. 5*G*,*I*, available at www.jneurosci.org as supplemental material). In addition, although FgfR3c-Fc treatment, which sequesters Fgf8-related signals, produced a slight increase in *Fgf15* expression, Fgf8 treatment itself did not suppress *Fgf15* expression (supplemental Fig. 5*G*,*H*, available at www.jneurosci.org as supplemental material). This raises the question of how Fgf8 and Fgf15/19 signals exert distinct outcomes in the subpallial differentiation from ESC-derived progenitors, even though both belong to the Fgf family. A structural comparison indicates that Fgf8 forms a subfamily with Fgf17 and Fgf18, whereas Fgf15/19 belongs to a separate subfamily that includes Fgf21 and Fgf23 (Itoh and Ornitz, 2004; Mason, 2007). In receptor–ligand binding (Ornitz et al., 1996; Zhang et al., 2006; Mason, 2007), Fgf8 shows a particularly high binding affinity for FGFR3c, whereas Fgf15/19 has a high affinity for FGFR2c and FGFR4. In addition to the differential effects on Nkx2.1/CoupTFII expression, Fgf8 caused a moderate increase in the pH3$^+$ percentage (mitotic index) within the SAG-treated telencephalic cells, whereas Fgf15/19 did not (supplemental Fig. 5*C*, available at www.jneurosci.org as supplemental material). Borello et al. (2008) also showed the Fgf8 and Fgf15 elicited distinct kinetics of ERK (extracellular signal-regulated kinase) and S6 phosphorylation. In the current study, when Fgf8 and Fgf15/19 were added together to culture, the Fgf8 phenotype dominated over the Fgf15/19-induced phenotype. Therefore, one possibility is that Fgf8 can activate a pathway in addition to the ones activated in common by Fgf8 and Fgf15/19.

Another unanswered question is whether the Fgf8 and Fgf15/19 signals also play distinct roles *in vivo* in the specification of the Nkx2.1$^+$ MGE domain. The *in vivo* expression domains of *Fgf8* and *Fgf15* in the rostral forebrain are mostly complementary (Borello et al., 2008): at E9.5, *Fgf15* is expressed in the anterior forebrain neuroepithelium, but is excluded from the anterior end (commissural plate), where *Fgf8* is expressed. At E12.5, unlike *Fgf8*, *Fgf15* is strongly expressed in the CGE and the preoptic area (weak expression is seen also in the pallial–subpallial boundary and the interganglionic sulcus). However, since genetic alteration of Fgf8 signaling in the mouse forebrain strongly affects the dorsal-ventral pattern of the telencephalon in addition to the impairing the rostral-caudal cortical pattern (Garel et al., 2003; Storm et al., 2006), this question is a rather complicated one requiring careful systematic analyses.

←

(*Figure legend continued.*) indicate the ventricular surface of the ganglionic eminences and the pial surface. ***I***, A high-magnification view of migrating Foxg1::venus$^+$ cells. ***J***, Foxg1::venus$^+$ cells migrating out of the cell mass. ***K***, Foxg1::venus$^+$ cells that have migrated into the lateral cortex (indicated in ***I***). Arrowheads, Neurites extending tangentially toward the dorsal cortex. ***L–O***, Adhesion culture of Foxg1::venus$^+$ cell aggregates cultured in MGE conditions. Foxg1::venus$^+$ cells were treated with 100 nM SAG after sorting, redissociated and replated on day 13, and fixed on day 35. Immunostaining with GFP (***L–N***), SOM (***L***), NPY (***M***), and PV (***N***) is shown. ***O***, Percentage of cells positive for SOM, NPY, and PV in Foxg1::venus$^+$ cells. Error bars indicate SEM. Scale bars: ***B***, ***C***, ***E***, ***J***, ***K***, 100 μm; ***G***, ***H***, 500 μm; ***I***, 200 μm; ***L–N***, 50 μm.

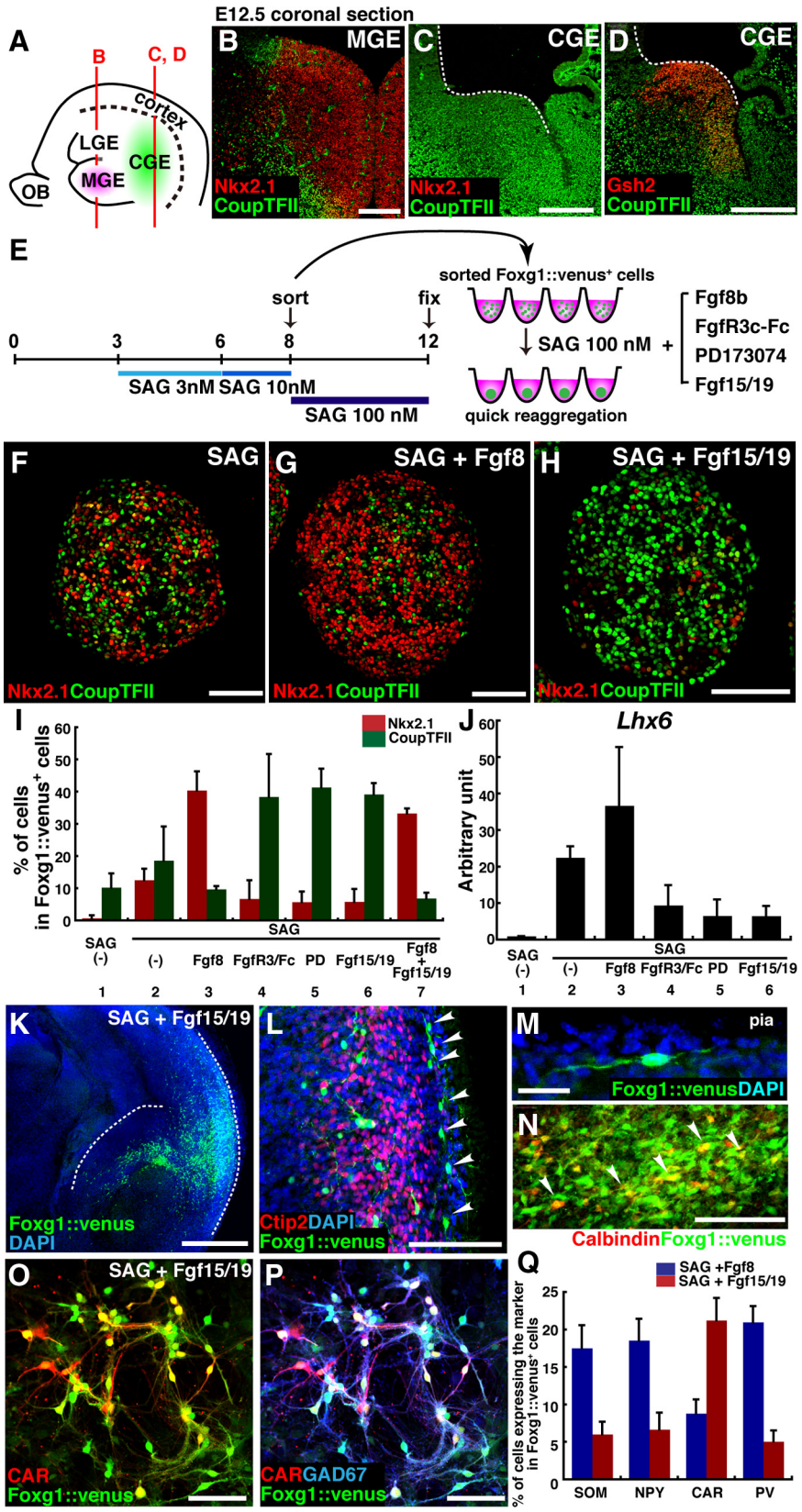

Figure 6. Fgf signals modulate the fate of SAG-induced ventral subpallial cells. ***A***, Schematic of the relative positions of the MGE and CGE in the sagittal view of the mouse telencephalon at E12.5. ***B–D***, Coronal sections of the mouse telencephalon at E12.5, immunostained with Nkx2.1/CoupTFII (***B***, ***C***) and CoupTFII/Gsh2 (***D***). ***E***, Fgf signaling affects MGE and CGE differentiation. ES cell aggregates were treated with SAG during days 3–6 (3 nM) and days 6–8 (10 nM) and were sorted on day 8. In addition to SAG (100 nM), sorted Foxg1::venus $^+$ cells were treated with Fgf8b (200 ng/ml), FgfR3c-Fc (100 ng/ml), PD173074 (10 nM), or Fgf15/19 (200 ng/ml). ***F–H***, Effects of Fgf8 and Fgf15/19 on the MGE marker Nkx2.1, and on the CGE marker CoupTFII. ***F***, SAG alone. ***G***, SAG and Fgf8b. ***H***, SAG and Fgf15/19. ***I***, Percentage of Nkx2.1 $^+$ and CoupTFII $^+$ cells in Foxg1::venus $^+$ cells. ***J***, qPCR analysis of the *Lhx6* expression in Foxg1::venus $^+$ cell aggregates on day 18. Each lane indicates the condition after sorting. ***K–N***, Immunostaining of a slice cocultured with a Foxg1::venus $^+$ cell reaggregate treated with SAG (100 nM) and Fgf15/19 (200 ng/ml) during days 8–12. ***K***, Foxg1::venus $^+$ cells migrating out of the reaggregate placed at the subventricular zone of the CGE. The dotted lines indicate the ventricular surface of the CGE and the pial surface. ***L***, Foxg1::venus $^+$ cells migrating in the marginal zone of the dorsal cortex (arrowheads). ***M***, A high-magnification view of a migrating Foxg1::venus $^+$ cell in the dorsal cortex. ***N***, Some of the Foxg1::venus $^+$ cells coexpressed calbindin (arrowheads). ***O***, ***P***, Dissociation adhesion culture of Foxg1::venus $^+$ cells that were treated with SAG (100 nM) and Fgf15/19 (200 ng/ml) after sorting. The cells were dissociated and replated on day 13 and fixed on day 25. Immunostaining with GFP (***O***, ***P***), CAR (***O***, ***P***), and GAD67 (***P***) is shown. ***Q***, Percentage of cells positive for SOM, NPY, CAR, and PV in Foxg1::venus $^+$ cells. For SOM, NPY, and CAR, cells were analyzed on day 25; for PV, cells were analyzed on day 35. Error bars indicate SEM. Scale bars: ***B–D***, 200 μm; ***F–H***, ***L***, ***O***, ***P***, 100 μm; ***K***, 500 μm; ***M***, ***N***, 20 μm.

Combination of SFEBq culture with FACS purification enables striatal neuronal grafting without forming tumors

Tumor formation is a large problem in transplanting ESC-derived neurons. The tumorigenesis associated with pluripotent cell applications falls into two categories: teratoma and nonteratoma (tissue type-specific) tumor formation. The latter can be caused by the contamination of lineage-restricted but immature stem cells.

In a previous report of striatal transplantation using Shh-treated human ESCs, nonteratoma tumors consisting of various neural-lineage cells were shown to form frequently. In contrast, tumor formation was not observed in our striatal transplantation of the FACS-sorted SFEBq cells, whereas tumors did form when FACS cell sorting was not performed (Fig. 4*J–U*; supplemental Fig. 4*D–J*, available at www.jneurosci.org as supplemental material).

In addition to successful striatal grafting, our preliminary transplantation study showed that interneurons generated from the SAG-treated (and SAG/Fgf8-treated) SFEBq cells integrated into the neocortex and occasionally expressed the interneuron markers SOM, NPY, PV, and CAR (supplemental Figs. 6, 7, available at www.jneurosci.org as supplemental material). As in the case of striatal grafting, the FACS-purified telencephalic (MGE/CGE) cells did not form tumors. The advantage of the intermediate FACS purification is also supported by a recent report (Maroof et al., 2010) in which ESC-derived interneurons puri-

fied with *Lhx6::GFP* labeling integrated into the cortical tissue without forming tumors.

Medium-sized spiny neurons are the main projection neurons that specifically degenerate in the early phase of Huntington's disease (Reiner et al., 1988). In addition, recent studies have shown that MGE-derived interneurons have suppressive effects on genetic epilepsy in mice (Alvarez-Dolado et al., 2006; Baraban et al., 2009). The nontumorigenic nature of the purified LGE/MGE derivatives generated *in vitro* from pluripotent cells, shown in this and other studies, should be advantageous for future medical applications.

References

Agoston DV, Szemes M, Dobi A, Palkovits M, Georgopoulos K, Gyorgy A, Ring MA (2007) Ikaros is expressed in developing striatal neurons and involved in enkephalinergic differentiation. J Neurochem 102:1805–1816.

Alvarez-Dolado M, Calcagnotto ME, Karkar KM, Southwell DG, Jones-Davis DM, Estrada RC, Rubenstein JL, Alvarez-Buylla A, Baraban SC (2006) Cortical inhibition modified by embryonic neural precursors grafted into the postnatal brain. J Neurosci 26:7380–7389.

Anderson SA, Eisenstat DD, Shi L, Rubenstein JL (1997) Interneuron migration from basal forebrain to neocortex: dependence on Dlx genes. Science 278:474–476.

Anderson SA, Marín O, Horn C, Jennings K, Rubenstein JL (2001) Distinct cortical migrations from the medial and lateral ganglionic eminences. Development 128:353–363.

Aubry L, Bugi A, Lefort N, Rousseau F, Peschanski M, Perrier AL (2008) Striatal progenitors derived from human ES cells mature into DARPP32 neurons in vitro and in quinolinic acid-lesioned rats. Proc Natl Acad Sci U S A 105:16707–16712.

Baraban SC, Southwell DG, Estrada RC, Jones DL, Sebe JY, Alfaro-Cervello C, García-Verdugo JM, Rubenstein JL, Alvarez-Buylla A (2009) Reduction of seizures by transplantation of cortical GABAergic interneuron precursors into Kv1.1 mutant mice. Proc Natl Acad Sci U S A 106:15472–15477.

Bolam JP, Hanley JJ, Booth PA, Bevan MD (2000) Synaptic organisation of the basal ganglia. J Anat 196:527–542.

Borello U, Cobos I, Long JE, McWhirter JR, Murre C, Rubenstein JL (2008) FGF15 promotes neurogenesis and opposes FGF8 function during neocortical development. Neural Dev 3:17.

Bulfone A, Kim HJ, Puelles L, Porteus MH, Grippo JF, Rubenstein JL (1993) The mouse Dlx-2 (Tes-1) gene is expressed in spatially restricted domains of the forebrain, face and limbs in midgestation mouse embryos. Mech Dev 40:129–140.

Bulfone A, Smiga SM, Shimamura K, Peterson A, Puelles L, Rubenstein JL (1995) T-brain-1: a homolog of Brachyury whose expression defines molecularly distinct domains within the cerebral cortex. Neuron 15:63–78.

Butt SJ, Fuccillo M, Nery S, Noctor S, Kriegstein A, Corbin JG, Fishell G (2005) The temporal and spatial origins of cortical interneurons predict their physiological subtype. Neuron 48:591–604.

Chang CW, Tsai CW, Wang HF, Tsai HC, Chen HY, Tsai TF, Takahashi H, Li HY, Fann MJ, Yang CW, Hayashizaki Y, Saito T, Liu FC (2004) Identification of a developmentally regulated striatum-enriched zinc-finger gene, Nolz-1, in the mammalian brain. Proc Natl Acad Sci U S A 101:2613–2618.

Chen JK, Taipale J, Young KE, Maiti T, Beachy PA (2002) Small molecule modulation of Smoothened activity. Proc Natl Acad Sci U S A 99:14071–14076.

Chiang C, Litingtung Y, Lee E, Young KE, Corden JL, Westphal H, Beachy PA (1996) Cyclopia and defective axial patterning in mice lacking Sonic hedgehog gene function. Nature 383:407–413.

Deacon TW, Pakzaban P, Isacson O (1994) The lateral ganglionic eminence is the origin of cells committed to striatal phenotypes: neural transplantation and developmental evidence. Brain Res 668:211–219.

Du T, Xu Q, Ocbina PJ, Anderson SA (2008) NKX2.1 specifies cortical interneuron fate by activating Lhx6. Development 135:1559–1567.

Eiraku M, Watanabe K, Matsuo-Takasaki M, Kawada M, Yonemura S, Matsumura M, Wataya T, Nishiyama A, Muguruma K, Sasai Y (2008) Self-organized formation of polarized cortical tissues from ESCs and its active manipulation by extrinsic signals. Cell Stem Cell 3:519–532.

Ferland RJ, Cherry TJ, Preware PO, Morrisey EE, Walsh CA (2003) Characterization of Foxp2 and Foxp1 mRNA and protein in the developing and mature brain. J Comp Neurol 460:266–279.

Flames N, Pla R, Gelman DM, Rubenstein JL, Puelles L, Marín O (2007) Delineation of multiple subpallial progenitor domains by the combinatorial expression of transcriptional codes. J Neurosci 27:9682–9695.

Flandin P, Kimura S, Rubenstein JL (2010) The progenitor zone of the ventral medial ganglionic eminence requires Nkx2–1 to generate most of the globus pallidus but few neocortical interneurons. J Neurosci 30:2812–2823.

Fuccillo M, Rallu M, McMahon AP, Fishell G (2004) Temporal requirement for hedgehog signaling in ventral telencephalic patterning. Development 131:5031–5040.

Fuccillo M, Joyner AL, Fishell G (2006) Morphogen to mitogen: the multiple roles of hedgehog signalling in vertebrate neural development. Nat Rev Neurosci 7:772–783.

Fukuchi-Shimogori T, Grove EA (2001) Neocortex patterning by the secreted signaling molecule FGF8. Science 294:1071–1074.

Garel S, Huffman KJ, Rubenstein JL (2003) Molecular regionalization of the neocortex is disrupted in Fgf8 hypomorphic mutants. Development 130:1903–1914.

Gaspard N, Bouschet T, Hourez R, Dimidschstein J, Naeije G, van den Ameele J, Espuny-Camacho I, Herpoel A, Passante L, Schiffmann SN, Gaillard A, Vanderhaeghen P (2008) An intrinsic mechanism of corticogenesis from embryonic stem cells. Nature 455:351–357.

Gorski JA, Talley T, Qiu M, Puelles L, Rubenstein JL, Jones KR (2002) Cortical excitatory neurons and glia, but not GABAergic neurons, are produced in the Emx1-expressing lineage. J Neurosci 22:6309–6314.

Gunhaga L, Jessell TM, Edlund T (2000) Sonic hedgehog signaling at gastrula stages specifies ventral telencephalic cells in the chick embryo. Development 127:3283–3293.

Hébert JM, Fishell G (2008) The genetics of early telencephalon patterning: some assembly required. Nat Rev Neurosci 9:678–685.

Hevner RF, Shi L, Justice N, Hsueh Y, Sheng M, Smiga S, Bulfone A, Goffinet AM, Campagnoni AT, Rubenstein JL (2001) Tbr1 regulates differentiation of the preplate and layer 6. Neuron 29:353–366.

Hsieh-Li HM, Witte DP, Szucsik JC, Weinstein M, Li H, Potter SS (1995) Gsh-2, a murine homeobox gene expressed in the developing brain. Mech Dev 50:177–186.

Ideguchi M, Palmer TD, Recht LD, Weimann JM (2010) Murine embryonic stem cell-derived pyramidal neurons integrate into the cerebral cortex and appropriately project axons to subcortical targets. J Neurosci 30:894–904.

Ishibashi M, McMahon AP (2002) A sonic hedgehog-dependent signaling relay regulates growth of diencephalic and mesencephalic primordia in the early mouse embryo. Development 129:4807–4819.

Itoh N, Ornitz DM (2004) Evolution of the Fgf and Fgfr gene families. Trends Genet 20:563–569.

Kanatani S, Yozu M, Tabata H, Nakajima K (2008) COUP-TFII is preferentially expressed in the caudal ganglionic eminence and is involved in the caudal migratory stream. J Neurosci 28:13582–13591.

Kohtz JD, Baker DP, Corte G, Fishell G (1998) Regionalization within the mammalian telencephalon is mediated by changes in responsiveness to Sonic Hedgehog. Development 125:5079–5089.

Lavdas AA, Grigoriou M, Pachnis V, Parnavelas JG (1999) The medial ganglionic eminence gives rise to a population of early neurons in the developing cerebral cortex. J Neurosci 19:7881–7888.

Leid M, Ishmael JE, Avram D, Shepherd D, Fraulob V, Dollé P (2004) CTIP1 and CTIP2 are differentially expressed during mouse embryogenesis. Gene Expr Patterns 4:733–739.

Li XJ, Zhang X, Johnson MA, Wang ZB, Lavaute T, Zhang SC (2009) Coordination of sonic hedgehog and Wnt signaling determines ventral and dorsal telencephalic neuron types from human embryonic stem cells. Development 136:4055–4063.

Long JE, Swan C, Liang WS, Cobos I, Potter GB, Rubenstein JL (2009a) Dlx1&2 and Mash1 transcription factors control striatal patterning and differentiation through parallel and overlapping pathways. J Comp Neurol 512:556–572.

Long JE, Cobos I, Potter GB, Rubenstein JL (2009b) Dlx1&2 and Mash1 transcription factors control MGE and CGE patterning and differentiation through parallel and overlapping pathways. Cereb Cortex 19 [Suppl 1]:i96–i106.

Lupo G, Harris WA, Lewis KE (2006) Mechanisms of ventral patterning in the vertebrate nervous system. Nat Rev Neurosci 7:103–114.

MacArthur CA, Lawshé A, Xu J, Santos-Ocampo S, Heikinheimo M, Chellaiah AT, Ornitz DM (1995) FGF-8 isoforms activate receptor splice forms that are expressed in mesenchymal regions of mouse development. Development 121:3603–3613.

Marin O, Rubenstein JL (2002) Patterning, regionalization and cell differentiation in the forebrain. In: Mouse development: patterning, morphogenesis, and organogenesis (Rossant J, Tam P, eds), pp 75–106. San Diego: Academic.

Maroof AM, Brown K, Shi SH, Studer L, Anderson SA (2010) Prospective isolation of cortical interneuron precursors from mouse embryonic stem cells. J Neurosci 30:4667–4675.

Mason I (2007) Initiation to end point: the multiple roles of fibroblast growth factors in neural development. Nat Rev Neurosci 8:583–596.

Mink JW (2008) The basal ganglia. In: Fundamental neuroscience, Ed 3 (Squire LR, Berg D, Bloom FE, du Lac S, Ghosh A, Spitzer NC, eds), pp 725–750. San Diego: Academic.

Miyoshi G, Butt SJ, Takebayashi H, Fishell G (2007) Physiologically distinct temporal cohorts of cortical interneurons arise from telencephalic Olig2-expressing precursors. J Neurosci 27:7786–7798.

Muguruma K, Nishiyama A, Ono Y, Miyawaki H, Mizuhara E, Hori S, Kakizuka A, Obata K, Yanagawa Y, Hirano T, Sasai Y (2010) Ontogeny-recapitulating generation and tissue integration of ES cell-derived Purkinje cells. Nat Neurosci 13:1171–1180.

Nery S, Fishell G, Corbin JG (2002) The caudal ganglionic eminence is a source of distinct cortical and subcortical cell populations. Nat Neurosci 5:1279–1287.

Ohkubo Y, Chiang C, Rubenstein JL (2002) Coordinate regulation and synergistic actions of BMP4, SHH and FGF8 in the rostral prosencephalon regulate morphogenesis of the telencephalic and optic vesicles. Neuroscience 111:1–17.

Olsson M, Campbell K, Wictorin K, Björklund A (1995) Projection neurons in fetal striatal transplants are predominantly derived from the lateral ganglionic eminence. Neuroscience 69:1169–1182.

Olsson M, Björklund A, Campbell K (1998) Early specification of striatal projection neurons and interneuronal subtypes in the lateral and medial ganglionic eminence. Neuroscience 84:867–876.

Ornitz DM, Xu J, Colvin JS, McEwen DG, MacArthur CA, Coulier F, Gao G, Goldfarb M (1996) Receptor specificity of the fibroblast growth factor family. J Biol Chem 271:15292–15297.

Ouimet CC, Langley-Gullion KC, Greengard P (1998) Quantitative immunocytochemistry of DARPP-32-expressing neurons in the rat caudatoputamen. Brain Res 808:8–12.

Porteus MH, Bulfone A, Liu JK, Puelles L, Lo LC, Rubenstein JL (1994) DLX-2, MASH-1, and MAP-2 expression and bromodeoxyuridine incorporation define molecularly distinct cell populations in the embryonic mouse forebrain. J Neurosci 14:6370–6383.

Rallu M, Machold R, Gaiano N, Corbin JG, McMahon AP, Fishell G (2002a) Dorsoventral patterning is established in the telencephalon of mutants lacking both Gli3 and Hedgehog signaling. Development 129:4963–4974.

Rallu M, Corbin JG, Fishell G (2002b) Parsing the prosencephalon. Nat Rev Neurosci 3:943–951.

Reiner A, Albin RL, Anderson KD, D'Amato CJ, Penney JB, Young AB (1988) Differential loss of striatal projection neurons in Huntington disease. Proc Natl Acad Sci U S A 85:5733–5737.

Shimamura K, Rubenstein JL (1997) Inductive interactions direct early regionalization of the mouse forebrain. Development 124:2709–2718.

Shimamura K, Hartigan DJ, Martinez S, Puelles L, Rubenstein JL (1995) Longitudinal organization of the anterior neural plate and neural tube. Development 121:3923–3933.

Skaper SD, Kee WJ, Facci L, Macdonald G, Doherty P, Walsh FS (2000) The FGFR1 inhibitor PD 173074 selectively and potently antagonizes FGF-2 neurotrophic and neurotropic effects. J Neurochem 75:1520–1527.

Storm EE, Garel S, Borello U, Hebert JM, Martinez S, McConnell SK, Martin GR, Rubenstein JL (2006) Dose-dependent functions of Fgf8 in regulating telencephalic patterning centers. Development 133:1831–1844.

Stoykova A, Gruss P (1994) Roles of Pax-genes in developing and adult brain as suggested by expression patterns. J Neurosci 14:1395–1412.

Stühmer T, Anderson SA, Ekker M, Rubenstein JL (2002) Ectopic expression of the Dlx genes induces glutamic acid decarboxylase and Dlx expression. Development 129:245–252.

Sussel L, Marin O, Kimura S, Rubenstein JL (1999) Loss of Nkx2.1 homeobox gene function results in a ventral to dorsal molecular respecification within the basal telencephalon: evidence for a transformation of the pallidum into the striatum. Development 126:3359–3370.

Toresson H, Potter SS, Campbell K (2000) Genetic control of dorsal-ventral identity in the telencephalon: opposing roles for Pax6 and Gsh2. Development 127:4361–4371.

Tripodi M, Filosa A, Armentano M, Studer M (2004) The COUP-TF nuclear receptors regulate cell migration in the mammalian basal forebrain. Development 131:6119–6129.

Watanabe K, Kamiya D, Nishiyama A, Katayama T, Nozaki S, Kawasaki H, Watanabe Y, Mizuseki K, Sasai Y (2005) Directed differentiation of telencephalic precursors from embryonic stem cells. Nat Neurosci 8:288–296.

Wataya T, Ando S, Muguruma K, Ikeda H, Watanabe K, Eiraku M, Kawada M, Takahashi J, Hashimoto N, Sasai Y (2008) Minimization of exogenous signals in ES cell culture induces rostral hypothalamic differentiation. Proc Natl Acad Sci U S A 105:11796–11801.

Wichterle H, Garcia-Verdugo JM, Herrera DG, Alvarez-Buylla A (1999) Young neurons from medial ganglionic eminence disperse in adult and embryonic brain. Nat Neurosci 2:461–466.

Wichterle H, Turnbull DH, Nery S, Fishell G, Alvarez-Buylla A (2001) In utero fate mapping reveals distinct migratory pathways and fates of neurons born in the mammalian basal forebrain. Development 128:3759–3771.

Wonders CP, Anderson SA (2006) The origin and specification of cortical interneurons. Nat Rev Neurosci 7:687–696.

Xu Q, Cobos I, De La Cruz E, Rubenstein JL, Anderson SA (2004) Origins of cortical interneuron subtypes. J Neurosci 24:2612–2622.

Xu Q, Wonders CP, Anderson SA (2005) Sonic hedgehog maintains the identity of cortical interneuron progenitors in the ventral telencephalon. Development 132:4987–4998.

Xu Q, Guo L, Moore H, Waclaw RR, Campbell K, Anderson SA (2010) Sonic hedgehog signaling confers ventral telencephalic progenitors with distinct cortical interneuron fates. Neuron 65:328–340.

Yozu M, Tabata H, Nakajima K (2005) The caudal migratory stream: a novel migratory stream of interneurons derived from the caudal ganglionic eminence in the developing mouse forebrain. J Neurosci 25:7268–7277.

Yun K, Potter S, Rubenstein JL (2001) Gsh2 and Pax6 play complementary roles in dorsoventral patterning of the mammalian telencephalon. Development 128:193–205.

Zhang X, Ibrahimi OA, Olsen SK, Umemori H, Mohammadi M, Ornitz DM (2006) Receptor specificity of the fibroblast growth factor family. The complete mammalian FGF family. J Biol Chem 281:15694–15700.